

Synthesis, Characterization, and Photophysical Properties of 2-Hydroxybenzaldehyde [(1*E*)-1-pyridin-2-ylethylidene]hydrazone and Its Rhenium(I) Complexes

Paula Barbazán,^[a] Rosa Carballo,^[a] Berta Covelo,^[a,b] Carlos Lodeiro,^[c] João Carlos Lima,^[c] and Ezequiel M. Vázquez-López*^[a]

Keywords: Rhenium / Hydrazones / Carbonyl ligands / Luminescence

The 2-hydroxybenzaldehyde [(1*E*)-1-pyridin-2-ylethylidene]hydrazone (HL²) ligand was prepared and its rhenium(I) complexes [ReX(CO)₃(HL²)] were obtained by reaction with *fac*-[ReX(CO)₃(CH₃CN)₂] (X = Cl, Br) in chloroform. The compounds were characterized by elemental analysis, mass spectrometry, and IR, UV/Vis, and ¹H NMR spectroscopy. Furthermore, the structures were also established by X-ray diffraction. The aromatic rings are almost coplanar in the ligand structure, and the configuration around the hydrazone group is strongly dominated by the presence of an intramo-

lecular hydrogen bond between the OH group and the hydrazinic nitrogen atom N1. The rhenium center is coordinated through the pyridine and hydrazinic nitrogen atoms to give a five-membered chelate ring. In addition, the free ligand shows interesting luminescence properties. The effect of the metal coordination on the photophysical behavior of the resulting complex was also studied.

(© Wiley-VCH Verlag GmbH & Co. KGaA, 69451 Weinheim, Germany, 2008)

Introduction

The study of rhenium(I) complexes with N,N'-chelate rings has two main aims. Firstly, the complexes of {Re(CO)₃}⁺ with N,N'-chelate ligands, in which one or both substituents are aromatic heterocycles, are exceptionally stable. There are numerous reports on complexes of this type as models for the design of ¹⁸⁸Re or ^{99m}Tc systems for therapeutic applications^[1] or labeling of targeting biomolecules.^[2–6] In the latter application, the selected ligand requires a second group for conjugation to a biomolecule. The kinetic inertness and chemical robustness of the complexes are also desirable properties for such applications. A second aspect of interest concerns the luminescent properties of the diimine complexes. Indeed, complexes of the type [ReCl(diimine)(CO)₃] with polypyridyls such as 2,2'-bipyridine as diimine ligands are generally luminescent.^[7] The emission originates from ³MLCT (triplet metal-to-ligand charge transfer excited states). Control of the photophysical properties of these complexes can be achieved by using a coligand with different ligand field strength to adjust the

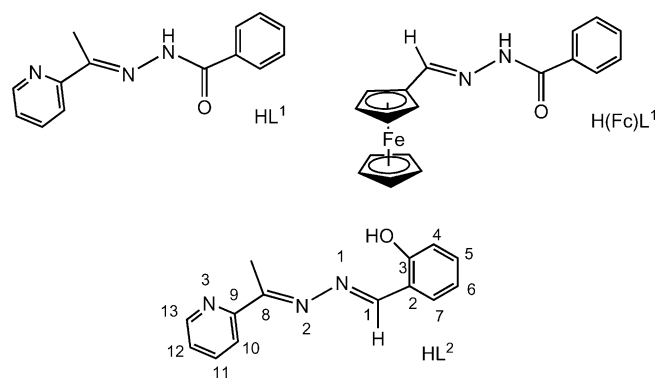
energy levels of the metal-centered dπ orbitals and/or by using functional groups that modulate the electron-donor or -acceptor properties of the ligands.^[8] Modifications may yield complexes that are no longer luminescent owing to the low energy of the MLCT states (energy-gap law^[9]), although in such cases other promising applications such as, for example, nonlinear optical properties may result.^[10]

We, in collaboration with other groups, have initiated a research program aimed at the synthesis and characterization of rhenium(I) complexes of different Schiff base derivatives like thiosemicarbazones^[11–13] and, more recently, hydrazone derivatives.^[14] Both series of ligands are versatile systems that can coordinate as neutral ligands or in their deprotonated form. In addition, different coordination groups can be easily added to the general framework in the search for different properties, such as those outlined above, or different coordinative behavior. For instance, HL¹ (Scheme 1) forms very stable complexes with the fragment *fac*-{ReX(CO)₃} (X = Br, H₂O) by N,N'-coordination.^[15] The substitution of the 2-acetylpyridine fragment by a formyl ferrocene group [H(Fc)L¹ in Scheme 1] gives rise to,^[16] as a result of the N,O-coordination mode, significant spectroscopic differences that may become suitable tools for coordinative diagnosis in the chemistry of hydrazone ligands. We present here the synthesis and characterization of an isomer of HL¹, 2-hydroxybenzaldehyde [(1*E*)-1-pyridin-2-ylethylidene]hydrazone (HL² in Scheme 1), for which appropriate photophysical properties derived from the salicylaldimine group^[17] are expected, despite the presence of the same donor groups as those in HL¹.

[a] Departamento de Química Inorgánica, Universidade de Vigo, Facultade de Química, 36310 Vigo, Galicia, Spain
Fax: +34-986-812556
E-mail: ezequiel@uvigo.es

[b] Unidade de Determinación Estructural e Proteómica, CACTI, Universidade de Vigo, 36310 Vigo, Spain

[c] REQUIMTE-CQFB, Departamento de Química, Facultade de Ciências e Tecnologia, Universidade Nova de Lisboa, 2829-516 Monte de Caparica, Portugal

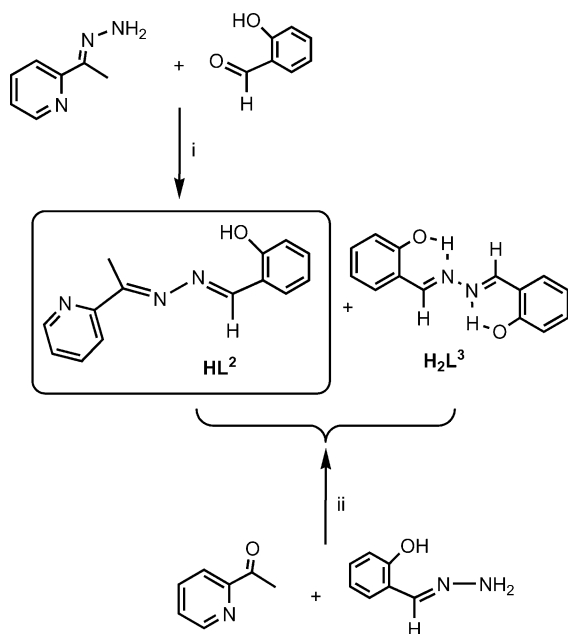


Scheme 1.

Results and Discussion

Synthesis and Spectroscopic Characterization

Ligand HL^2 was readily obtained by reaction of the previously prepared 2-acetylpyridine hydrazone with salicylaldehyde as described previously (Scheme 2, path i).^[18] Elemental analysis and spectroscopic characterization support the formation of the ligand. X-ray quality crystals of the free ligands were obtained by slow evaporation of the mother liquor.

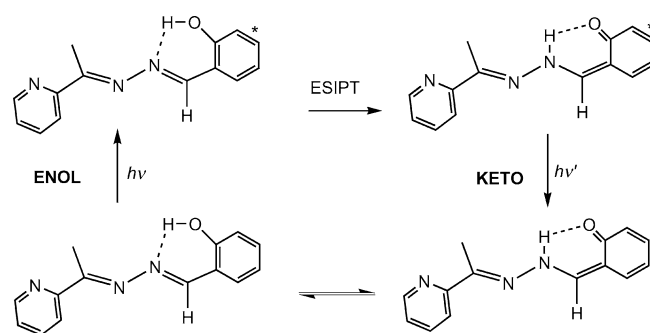


Scheme 2.

Another possible path (Scheme 2, path ii) for the synthesis of the target compound from commercial salicylaldehyde hydrazone was also explored. In this case, the ligand was obtained in very low yield, which did not increase upon use of other solvents or reaction conditions (ethanol, toluene, or catalytic amounts of sulfuric or hydrochloric acids or by using water-trapping systems, such as a Dean–Stark receiver). Interestingly, we observed the formation of bis(2-hydroxybenzaldehyde)hydrazone (H_2L^3 , Scheme 2) in reactions through path ii, and in fact, this was the major prod-

uct in some instances. The formation of this unexpected compound was proved by spectroscopic studies (IR, NMR, mass spectrometry, and X-ray diffraction)^[19] and can only be avoided by following path i.

The formation of H_2L^3 (Scheme 3) from salicylaldehyde hydrazone in the presence of $[\text{W}(\text{CO})_6]$ was described before.^[20] The authors propose the formation of a dimer by attack of a molecule of salicylaldehyde hydrazone on its tungsten complex. The tetracyclic intermediate, $\text{N}-\text{NH}_2-\text{NH}_2-\text{N}$, yields the bis(2-hydroxybenzaldehyde)hydrazone through decomposition of the metal complex after release of hydrazine. Although this mechanism is probably correct, our observation of the formation of H_2L^3 in the synthesis of HL^2 provides evidence against the catalytic role attributed to $[\text{W}(\text{CO})_6]$ or other metals. In fact, the rhenium(I) complexes were obtained in good yield and the formation of H_2L^3 from its solutions was not observed in any case (see below).

Scheme 3. Mechanism of excited-state intramolecular proton transfer (ESIPT) responsible for the fluorescence in HL^2 .

The *fac*- $[\text{ReX}(\text{HL}^2)(\text{CO})_3]$ (**1**, $\text{X} = \text{Cl}$; **2**, $\text{X} = \text{Br}$) complexes were obtained as reddish-brown solids in high yield by reaction of 1:1 mixtures of HL^2 and *fac*- $[\text{ReX}(\text{CO})_3-(\text{CH}_3\text{CN})_2]$ in refluxing chloroform. We attempted to obtain the complexes from the corresponding 2-acetylpyridine rhenium complex by following a similar method to that reported by Alberto et al.^[21] for the synthesis of rhenium(I) complexes of different Schiff base ligands, but the title compounds were not detected. Elemental analysis and mass spectrometry confirmed the stoichiometry. A facial geometry around the rhenium atom is suggested by the three strong $\nu(\text{CO})$ IR bands in the range 1901–2036 cm^{-1} .

In the ^1H NMR spectra of both isolated rhenium(I) complexes in $[\text{D}_6]\text{DMSO}$, the C–H proton signals are generally shifted to lower field with respect to that of the free ligand (HL^2). This effect of rhenium coordination was also observed in other hydrazine-based ligands such as thiosemicarbazones.^[11–15] However, metalation has the opposite effect on the H–O signal. Bearing in mind that the hydrogen bond is probably responsible for the strong displacement ($\delta = 11.40$ ppm) of the H–O signal in free HL^2 with respect to the usual position for an aromatic alcohol, the chemical shift observed in the complexes ($\delta = 10.50$ ppm) suggests a different electronic distribution on the hydroxybenzylidene

hydrazone fragment induced by the metal fragment. However, conclusions based on the differences in the ^1H chemical-shift data for the hydroxy group between the ligand and its complexes are unreliable, because although the resonances of the hydroxy protons involved in the hydrogen bonds tend to be shifted downfield, they are subject to numerous effects that are hard to predict.^[22] In contrast, the $d\delta/dT$ values of hydroxy groups do provide some information about intramolecular hydrogen bonding. Strongly hydrogen-bonded hydroxy groups show little change with temperature, because the interaction with solvents that are hydrogen-bond acceptors is small. Conversely, the chemical shifts of hydroxy protons hydrogen bonded to the solvent do show a marked temperature dependence due to changes in mobility of the solvent molecules.^[23] The $d\delta/dT$ values for the rhenium complexes (6×10^{-3} ppm) are almost twice the value of the free ligand (4×10^{-3} ppm), but they suggest that, although the hydrogen bond is probably weakened, the hydroxy proton is mainly involved in the intramolecular interaction – a situation consistent with solid-state results (see below).

X-ray Studies

The molecular structures and the numbering scheme of the free ligand and the rhenium complexes included in the present work are shown in Figure 1. Selected bond lengths and angles are included in Table 1. Details about the data collection and refinement are included in the Experimental Section.

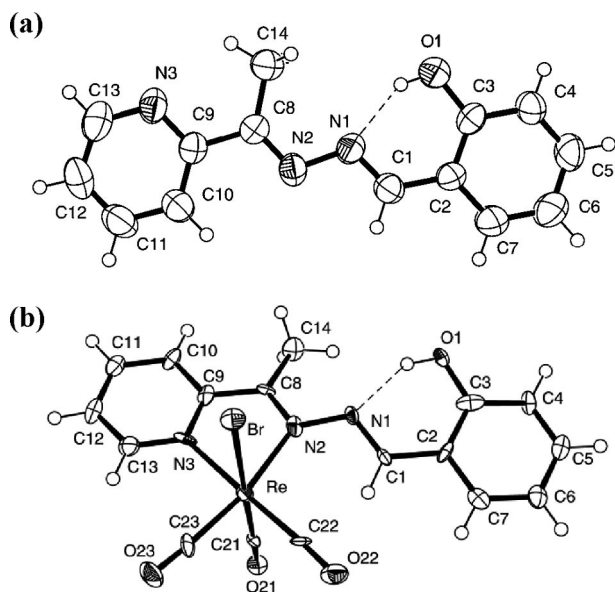


Figure 1. Molecular structure of HL^2 (A) and $[\text{ReBr}(\text{CO})_3(\text{HL}^2)]$ (B).

The structure of HL^2 was obtained from single crystals formed from the mother liquor. The study by X-ray diffraction of red single crystals of the compounds $[\text{ReX}(\text{CO})_3\{\text{HL}^2\}]$ showed them to be isotypic and confirmed the metal configuration inferred from the spectroscopic data.

Table 1. Main interatomic distances [\AA] and angles [$^\circ$] in HL^2 , $[\text{ReCl}(\text{CO})_3(\text{HL}^2)]$ (1), and $[\text{ReBr}(\text{CO})_3(\text{HL}^2)]$ (2).

	HL^2	1	2
O1–C3	1.351(4)	1.356(8)	1.346(12)
N2–C8	1.278(4)	1.280(9)	1.323(13)
N2–N1	1.408(4)	1.402(7)	1.387(10)
N1–C1	1.268(4)	1.298(9)	1.289(13)
C8–C9	1.473(5)	1.475(9)	1.457(14)
C2–C1	1.449(5)	1.439(9)	1.447(13)
Re–N3		2.152(6)	2.154(9)
Re–N2		2.222(6)	2.203(9)
Re–Cl		2.493(2)	
Re–Br			2.6257(11)
C8–N2–N1	113.4(3)	113.3(6)	111.8(9)
C1–N1–N2	113.9(3)	117.2(6)	115.4(9)
N2–C8–C9	116.5(3)	117.1(7)	116.6(9)
N2–C8–C14	125.4(4)	123.8(7)	122.5(10)
N1–C1–C2	123.0(4)	122.4(7)	122.1(9)
N3–Re–N2		73.3(2)	73.8(3)
C8–N2–Re		117.6(5)	116.5(7)
N1–N2–Re		129.1(4)	131.6(7)
C9–N3–Re		118.4(5)	118.2(7)
N3–C9–C8	116.3(4)	113.5(6)	114.8(10)

The two aromatic rings in the structure of the HL^2 ligand are practically coplanar. The configurations of the bonds involved in the hydrazone group are strongly dominated by the hydrogen bonding between the OH group and the nitrogen N1 atom. This interaction yields a very stable six-membered ring,^[24] which is also observed in the two rhenium complex structures and, in addition, is responsible for the *E* configuration of the $\text{C1}=\text{N1}$ bonds in the three compounds. The configuration of the $\text{N2}=\text{N1}$ and $\text{C8}=\text{N2}$ bonds is also *E* in HL^2 .

The coordination polyhedron around the rhenium atom can be described as a distorted octahedron formed by coordination of the two nitrogen atoms of the HL^2 ligand, N2 and N3, by the three carbonyl carbon atoms and the halogen atoms. The main distortion from the ideal octahedral geometry is imposed by the formation of a chelate ring, as can be seen by the N2–Re–N3 angle (Table 1). The Re–N and Re–X distances are similar to those found in complexes of the fragment *fac*-“ $\text{ReX}(\text{CO})_3$ ” with hydrazone-based ligands,^[25] for example, $[\text{ReBr}(\text{CO})_3(\text{HL}^1)]$ (2.158 and 2.167 \AA).^[15]

The phenyl and pyridine rings are also coplanar after coordination, as can be deduced from angle between the root mean square planes of 15.4(3) and 13.6(3) $^\circ$ for compounds 1 and 2, respectively [3.0(1) $^\circ$ for HL^2]. The coordination of the rhenium to the N2 and N3 atoms and, consequently, the formation of the five-membered chelate ring, lead to rotation of the pyridine ring with respect to that in HL^2 (where the N3 atom is oriented towards the methyl group C14). In terms of the bond lengths in the hydrazone arm, there are only statistical differences between the values observed in free ligand and its complex.

An interesting parameter that highlights differences between the free ligand and its complexes is the intramolecular hydrogen bond. We allowed the hydroxy hydrogen atom to refine freely in order to obtain more metric information

on the D–H···A values. Although the differences between the O1–H and H···N1 distances and the O1–H···N1 angle are not significant due to the high value of the standard deviation associated with them, the lengthening of the O1···N1 distance is reliable (Table 2). In the free ligand, the O1–H···N1 parameters indicate a significant hydrogen-bonding interaction. The O1···N1 distance is borderline between a strong and normal (moderate) hydrogen bond.^[26] However, the quality of the crystals of the complexes and, consequently, the high values of the standard deviation did not allow precise information to be obtained on the H···N1 and O1–H···N1 distances and angles. Once again, the O1···N1 distance, although longer than that observed in the free ligand, indicates a moderate hydrogen bond. The angle between the plane defined by the atoms C8–N2–N1 and the phenoxy group plane is almost negligible in HL² (1.3°) but increases to 19.5° in **1** and 17.2° in **2**.

Table 2. Structural parameters describing intramolecular and intermolecular moderate and nonconventional hydrogen bonds.^[a]

D–H···A	<i>d</i> (D–H) [Å]	<i>d</i> (H···A) [Å]	<i>d</i> (D···A) [Å]	<(DHA) [°]
HL ²				
O1–H1···N1	0.98(3)	1.69(3)	2.598(2)	153(2)
C1–H2···O1 ^{#1}	0.93	2.60	3.462(3)	155.4
C11–H11···N3 ^{#2}	0.93	2.75	3.589(3)	151.3
1				
O1–H1···N1	0.84(8)	1.97(9)	2.635(7)	135(8)
C10–H10···Cl ^{#3}	0.95	2.85	3.754(8)	161.8
C11–H11···O1 ^{#4}	0.95	2.466	3.384(10)	175.3
2				
O1–H1···N1	0.70(10)	2.17(11)	2.645(11)	126(12)
C10–H10···Br ^{#3}	0.93	2.96	3.858(11)	163.8
C11–H11···O1 ^{#4}	0.93	2.42	3.347(15)	172.5

[a] Symmetry code #1 $x - 1/2, -y + 1/2, -z + 1$; #2 $x - 1/2, y, -z + 1/2$; #3 $1 - x, -y, -z$; #4 $1 - x, 1/2 + y, -1/2 - z$.

The intermolecular association in the structures of the HL² ligand and the two rhenium complexes is shown in Figure 2. As outlined above, the OH group is prevented from establishing hydrogen-donor intermolecular interactions, because of the strong *intramolecular* interaction with the N1 atom, although it can interact with H atoms of C–H aromatic groups to link the molecules into chains (Figure 2a). In the structure of HL², these chains are associated through weak zig-zag C–H···N or C_{methyl}–H··· π interactions in the characteristic herringbone arrangement usually observed when the latter kind of interaction is present in aromatic molecules.^[27] This type of arrangement gives rise to zig-zag sheets (Figure 2b).

The intermolecular associations in the structures of complexes **1** and **2** can be described in two steps. Firstly, the molecules are associated in centrosymmetric dimers through C10–H···X^{#3} interactions. Although the C–H···X distances are slightly longer than those usually reported,^[28] they are shorter than the sum of the van der Waals radii. In addition, the distances reported previously were observed in systems with interactions between organic fragments and anionic Cl[−] or Br[−]. In fact, a systematic study of these pa-

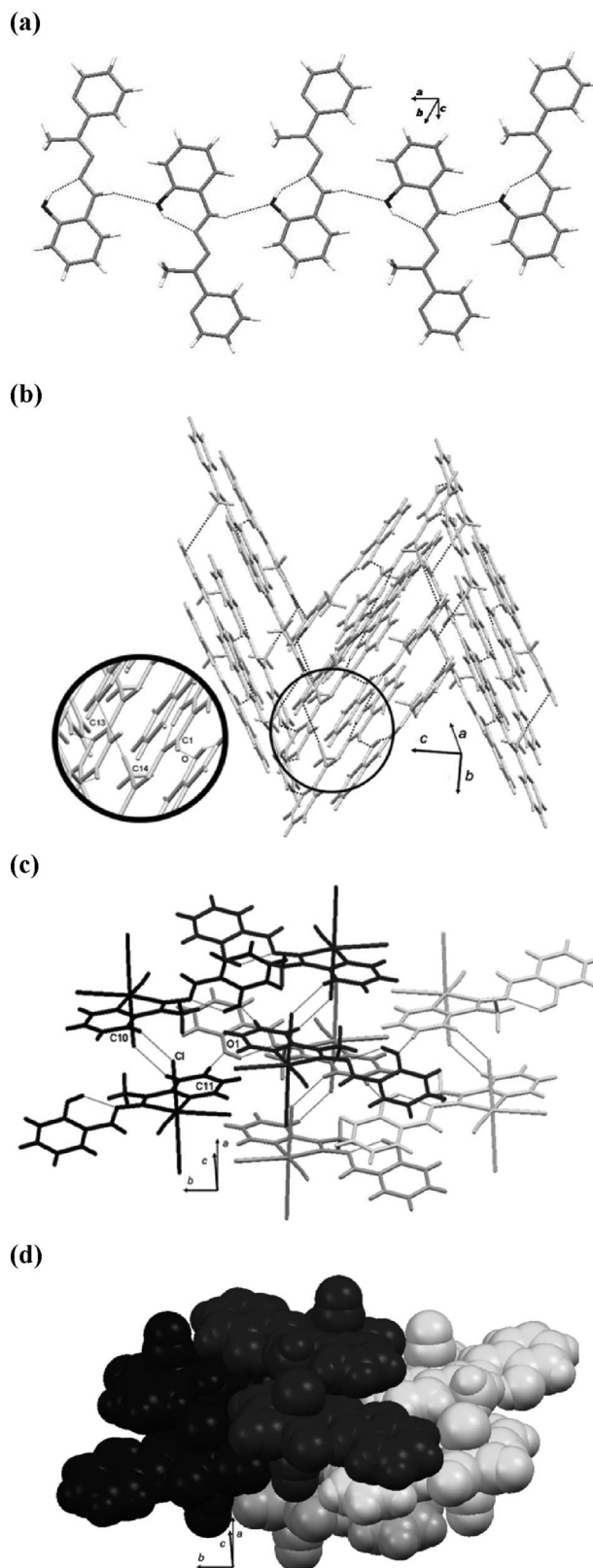


Figure 2. Intermolecular associations in the structure of HL² (a), (b) and **1** and **2** (c), (d).

rameters in M–X groups has yet to be carried out. Secondly, the dimers are associated in a brick-wall arrangement through C11–H···O1^{#4} interactions (Figure 2c and d).

Note that the C–H···O intermolecular interaction is reinforced in the complexes with respect to the free ligand (Table 2). However, it does not seem to be responsible of the lengthening of the intramolecular interaction N···H–O. The NMR spectroscopic solution studies, where the C–H···O interaction is absent, suggest that the last interaction is weaker in the complexes than in HL².

UV/Vis Absorption and Emission Spectra

The free-ligand UV/Vis absorption spectrum (Figure 3a) is characterized by two bands at 342 and 295 nm, which

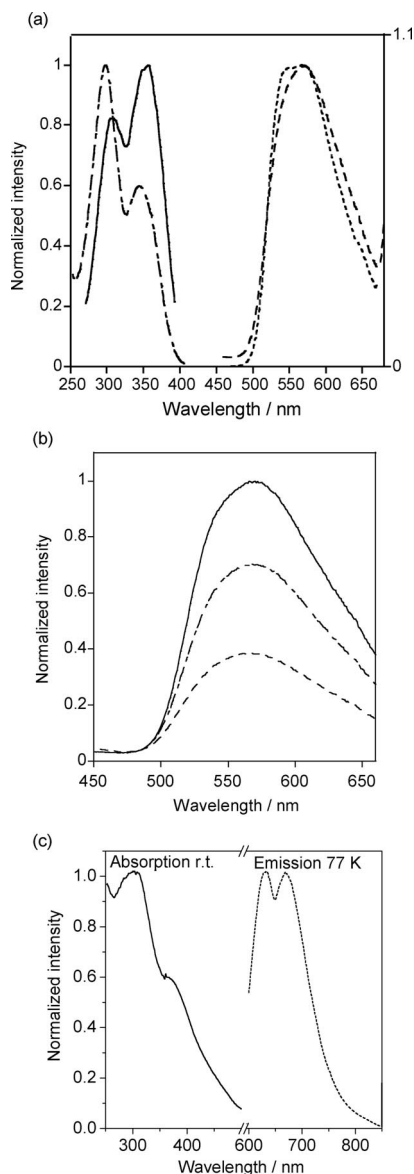


Figure 3. (a) Absorption (– – –) and emission (—) of HL² in chloroform solution ([HL²] = 2.1 × 10^{−5} M, 25 °C, λ_{exc} = 345 nm), emission spectra of HL² in the solid state (----), and excitation spectra collecting at λ_{em} = 560 nm (—); (b) fluorescence emission spectra of HL² in chloroform (—), methanol (– – –), and 50:50 v/v mixture chloroform/methanol (– · –) solutions. ([L] = 2.1 × 10^{−5} M, 25 °C, λ_{exc} = 345 nm); (c) absorption spectra of complex 2 in chloroform (2.1 × 10^{−5} M, λ_{exc} = 370 nm) at 25 °C (—), and emission spectra at 77 K for complex 2 in chloroform (····).

are due to π–π* transitions of the hydrazone group. The absorption spectra of both complexes (Figure 3b) are identical and show broader bands that are redshifted relative to those in the free ligand: ca. 373 nm (shoulder) and 301 nm. The longest wavelength band has a tail up to around 450 nm and this is responsible for the orange coloration of both complexes.

The free ligand has fluorescent properties that are apparent under a UV lamp (λ = 365 nm). The emission spectra of the HL² ligand (CHCl₃ solution and solid state at room temperature) are shown in Figure 3a. The maximum of the emission band in chloroform presents an exceptionally large Stokes' shift (11.027 cm^{−1} = 31.5 kcal/mol) similar to those found in other molecules with the salicylaldehyde group and usually assigned to an excited-state intramolecular proton transfer state (ESIPT) present in these molecules.^[29] The intensity of the fluorescence emission of HL² decreases considerably when a protic solvent such as methanol is added to the chloroform solution (Figure 3b; Table 3) with no noticeable change in the emission maximum. This is due to the competition for intermolecular hydrogen bonding from the solvent, which destabilizes the intramolecular hydrogen bond in the molecule – a feature that is necessary for the occurrence of intramolecular proton transfer. Both aspects confirm that the emission is due to de-excitation of an excited state of the keto form of the salicylaldehyde group (Scheme 3).^[17]

Table 3. UV/Vis absorption data for the free ligand and its rhenium(I) complexes.

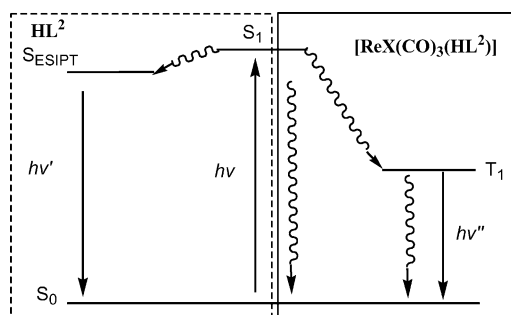
Compound	Solvent	λ [nm] (ε [L/mol cm])
HL ²	CHCl ₃	342 (14148), 295 (23646)
	MeOH	344 (16500), 296 (27300)
1	CHCl ₃	301 (21487), 373 (37526)
	MeOH	352 (19100), 284 (27100)
2	CHCl ₃	304 (8900), 378 (15081)
	MeOH	368 (53433), 276 (89130)

Both rhenium(I) complexes are nonemissive at room temperature. The increase in intersystem crossing due to the presence of the metal deactivates efficiently the singlet excited state and fluorescence is no longer observed. Triplet emission is also strongly quenched at room temperature. In contrast, when dichloromethane solutions of [ReBr(CO)₃-(HL²)] are cooled to 77 K, a weak redshifted emission with vibrational structure (maxima at 630 at 670 nm) is detected (Figure 3b) and is assigned to a triplet state.

Conclusions

The photophysical properties of the studied compounds are of interest. The mechanism shown in Scheme 3 for the fluorescence of HL² has been proposed for other luminescent systems based on Schiff bases of salicylaldehyde with amines,^[29] and the luminescent behavior of these systems is very sensible to changes in the N···H–O interactions such as electron density on the hydrogen-bonding acceptor or the planarity of the molecule. Both factors are affected by

rhodium coordination, as observed in the solid state (*X*-ray studies) and $d\delta/dT$ values of NMR hydroxy signals suggest similar behavior in solution, and contribute to the deactivation of ES IPT mechanism in the complexes. Thus, the behavior observed in **2** involves emission at low temperature and at wavelengths higher than in the fluorescence spectrum of the free ligand, and furthermore, the emission band presents vibration resolution – an observation consistent with an emission process from a low-energy triplet state (a summary of the processes is illustrated in Scheme 4). Similar behavior was observed in other rhodium(I) complexes.^[30] As in those cases, collisions with solvent molecules at room temperature favor de-excitation by vibrational relaxation as opposed to radiative decay from the forbidden $T_1 \rightarrow S_0$ transition. When the former path is deactivated (low temperature and/or rigid medium), then phosphorescence can be observed.



Scheme 4. Energy-level diagram for the emitting state of HL^2 (dotted box) and its rhodium(I) complexes. Ligand emission is derived from an excited-state intramolecular proton transfer (ESIPT) state, whereas the complex emission (only observed at 77 K) is derived from a ligand-centered triplet state.

Experimental Section

General: All operations performed in the synthesis and isolation of the compounds were carried out under an atmosphere of dry argon. All solvents were dried with appropriate drying agents, degassed by using a vacuum line, and distilled under an Ar atmosphere. $[ReX(CO)_5]$ ^[31] and $[ReX(CO)_3(CH_3CN)_2]$ ^[32] were prepared as previously reported. 2-Acetylpyridine, hydrazine hydrate, and salicylaldehyde were purchased from Aldrich. Elemental analyses were carried out with a Fisons EA-1108. Although the microanalysis results for rhodium compounds are clearly enhanced by addition of combustion catalyst (V_2O_5), the carbon results are without $\pm 0.4\%$. However, inspection of the ^{13}C NMR spectra shows exclusively signals attributed to the compounds. Melting points were determined with a Gallenkamp MFB-595 apparatus and are uncorrected. Mass spectra were recorded with a Hewlett-Packard 5989A spectrometer operating under FAB conditions (nitrobenzyl alcohol matrix). IR spectra were recorded from KBr pellets with a Bruker Vector 22FT. 1H NMR spectra were obtained with a Bruker AMX 400 spectrometer from $[D_6]DMSO$ solutions. UV/Vis spectra were obtained with a CARY 100 BIO (Varian) spectrophotometer from MeOH and $CHCl_3$ solutions. Fluorescence emission spectra were measured with a Horiba-Jobin-Yvon SPEX Fluorolog 3.22 spectrofluorimeter with a spectral band width of 5.0 nm for excitation and emission spectra. Steady-state fluorescence emission measure-

ments were also recorded in the solid state by using an optical fiber device connected to the spectrofluorimeter. The decay times of the compounds were too fast for the equipment time resolution (<100 ps). The quantum yields were also very low ($\leq 1.5 \times 10^{-3}$) and with significant error.

X-ray Crystallography: Crystallographic data collection and refinement parameters are listed in Table 4. All crystallographic measurements were performed with a Bruker Smart CCD apparatus at CACTI (University of Vigo) at room temperature [293(2) K] by using graphite monochromated Mo- K_α radiation ($\lambda = 0.71073$ Å). The data were corrected for absorption effects by using the SADABS program.^[33] Structure analyses were carried out by direct methods.^[34] Least-squares full-matrix refinements on F^2 were performed by using the SHELXL97 program. Atomic scattering factors and anomalous dispersion corrections for all atoms were taken from *International Tables for Crystallography*.^[35] All non-hydrogen atoms were refined anisotropically. Hydrogen atoms were refined as riders except O1-H, which was refined isotropically at positions previously identified in the corresponding Fourier map. Graphics were obtained with PLATON^[36] and MERCURY.^[37]

Table 4. Crystal data collection and structure refinement data.

Compound	HL^2	1	2
Formula	$C_{14}H_{13}N_3O$	$C_{17}H_{13}ClN_3O_4Re$	$C_{17}H_{13}BrN_3O_4Re$
M_r	239.27	544.95	589.41
Crystal system	orthorhombic	monoclinic	monoclinic
Space group	$P2_1/c$	$P2_1/c$	$P2_1/c$
a [Å]	12.375(3)	14.8520(16)	14.915(2)
b [Å]	13.306(3)	16.5924(18)	16.541(2)
c [Å]	15.091(3)	7.0420(7)	6.9455(9)
β [°]		93.779(2)	92.838(2)
V [Å ³]	2485.1(10)	1731.6(3)	1711.4(4)
Z	8	4	4
D_c	1.274	2.090	2.288
$S^{[a]}$	0.784	0.801	0.811
$R^{[b,c]}$	0.0491	0.0398	0.0501
$wR_2^{[b,d]}$	0.0836	0.0691	0.0780
Max./min. peaks [e Å ⁻³]	0.222/−0.284	1.316/−1.418	1.573/−2.271

[a] Goodness-of-fit on F^2 . [b] Observation criterion $I > 2\sigma(I)$. [c] $R = \sum ||F_o| - |F_c|| / \sum |F_o|$. [d] $wR_2 = \{\sum [w(F_o^2 - F_c^2)^2] / \sum [w(F_o^2)^2]\}^{1/2}$.

CCDC-666491 (for HL^2), -666492 (for **1**), and -666493 (for **2**) contain the supplementary crystallographic data for this paper. These data can be obtained free of charge from The Cambridge Crystallographic Data Centre via www.ccdc.cam.ac.uk/data_request/cif.

Synthesis of HL^2 : 2-Acetylpyridine hydrazone was synthesized by following the method reported by Sandbhor et al.^[38] with a slight modification as follows: to a solution of hydrazine hydrate (7.8 mL, 8026 mg) in methanol (25 mL) was added 2-acetylpyridine (1.12 mL, 1209.6 mg), and the solution was stirred at 0 °C for 2 h. The pale-yellow solution was stored in the refrigerator overnight. The solvent was removed in vacuo to 10 mL, and the pale-yellow precipitate was filtered off and dried under vacuum over $CaCl_2/KOH$. A solution of salicylaldehyde (0.03 mL, 34.38 mg) in methanol (5 mL) was added dropwise to a solution of the crude material (100 mg) in methanol (10 mL). The yellow solution was heated (30–40 °C) for 2 h. The yellow precipitate was filtered off and dried under vacuum over $CaCl_2/KOH$. Single crystals of HL^2 were obtained from the mother liquor. Yield: 76 mg (86%). M.p. 140 °C. 1H NMR: $\delta = 11.40$ (s, 1 H, O1-H), 8.90 (s, 1 H, C1-H), 8.70 (d, $J = 4.090$ Hz, 1 H, C13-H), 8.20 (d, $J = 7.998$ Hz, 1 H, C10-H), 7.90 (t, $J = 7.737$ Hz, 1 H, C11-H), 7.70 (d, $J = 7.602$ Hz, 1 H, C7-

H), 7.50 (t, $J = 6.041$ Hz, 1 H, C12-H), 7.40 (t, $J = 7.727$ Hz, 1 H, C5-H), 7.00 (m, 2 H, C4,6-H), 2.52 (s, 3 H, C14-H) ppm. ^{13}C RMN: $\delta = 165.72$ (C3), 161.04 (C1), 158.69 (C8), 154.43 (C9), 148.91 (C13), 136.68 (C11), 133.02 (C5), 131.05 (C7), 125.07 (C12), 120.87 (C10), 119.46 (C6), 118.39 (C2), 116.36 (C4), 13.67 (C14) ppm. IR: $\tilde{\nu} = 3444$ [s, br. $\nu(\text{OH})$], 1618 (s), 1547 (w), 1462 [m $\nu(\text{C}=\text{N}) + \nu(\text{C}=\text{C})$], 1272–1029 [m, w $\delta(\text{C}-\text{H})$] cm^{-1} . MS: m/z (%) = 240.01 (100) $[\text{M}]^+$. $\text{C}_{14}\text{H}_{13}\text{N}_3\text{O}$ (239.28): calcd. C 70.28, H 5.48, N 17.56; found C 70.05, H 5.46, N 17.61.

Synthesis of the $[\text{ReX}(\text{CO})_3(\text{HL}^2)]$ (1, X = Cl; 2, X = Br) Complexes:

To a solution of HL^2 (31.0 mg X = Cl or 27.2 mg X = Br) in CHCl_3 (10 mL) was added the corresponding equimolecular amount of *fac*- $[\text{ReX}(\text{CO})_3(\text{CH}_3\text{CN})_2]$ (50.4 mg X = Cl, 49.0 mg X = Br), and the red solution/mixture was heated under reflux for 2 h. The red-brown precipitate was filtered off and dried under vacuum. Single crystals suitable for X-ray studies were obtained by slow evaporation of ethyl acetate (for 1) or chloroform (for 2) solutions. Data for 1: Yield: 47.1 mg (66.7%). M.p. 261 °C. ^1H NMR: $\delta = 10.50$ (s, 1 H, O1-H), 9.20 (s, 1 H, C1-H), 9.00 (d, $J = 5.226$ Hz, 1 H, C13-H), 8.40 (m, 2 H, C10,11-H), 8.00 (d, $J = 7.831$ Hz, 1 H, C7-H), 7.80 (t, $J = 6.308$ Hz, 1 H, C12-H), 7.45 (t, $J = 8.539$ Hz, 1 H, C5-H), 7.00 (m, 2 H, C4,6-H), 2.60 (s, 3 H, C14-H) ppm. ^{13}C RMN: $\delta = 197.32$, 196.82 (C15,17), 187.83 (C16), 168.88 (C3), 158.63 (C1), 157.74 (C8), 154.86 (C9), 152.98 (C13), 140.18 (C11), 134.39 (C5), 128.85 (C7), 127.59 (C12), 127.32 (C10), 119.61 (C6), 117.94 (C2), 116.59 (C4), 15.59 (C14) ppm. IR: $\tilde{\nu} = 3446$ [m, br. $\nu(\text{OH})$], 2034 (m), 1902 [s $\nu(\text{CO}_{\text{fac}})$], 1623 (w), 1603 (w), 1568 (w), 1537 (w), 1484 [w $\nu(\text{C}=\text{N}) + \nu(\text{C}=\text{C})$], 1267–1039 [w $\delta(\text{C}-\text{H})$] cm^{-1} . MS: m/z (%) = 544.92 (21.41) $[\text{M}]^+$, 509.95 (29.42) $[\text{M} - \text{Cl}]^+$, 425.97 (3.51) $[\text{M} - 3\text{CO}]^+$. $\text{C}_{17}\text{H}_{13}\text{ClN}_3\text{O}_4\text{Re}$ (544.97): calcd. C 37.47, H 2.40, N 7.71; found C 36.87, H 2.31, N 7.53. Data 2: Yield: 49.6 mg (74.2%). M.p. 289 °C. ^1H NMR: $\delta = 10.50$ (s, 1 H, O1-H), 9.20 (s, 1 H, C1-H), 9.00 (d, $J = 5.221$ Hz, 1 H, C13-H), 8.40 (d, $J = 7.980$ Hz, 1 H, C10-H), 8.30 (t, $J = 5.2720$ Hz, 1 H, C11-H), 8.00 (d, $J = 7.707$ Hz, 1 H, C7-H), 7.80 (t, $J = 5.8925$ Hz, 1 H, C12-H), 7.40 (t, $J = 8.0475$ Hz, 1 H, C5-H), 7.00 (m, 2 H, C4,6-H), 2.70 (s, 3 H, C14-H) ppm. ^{13}C RMN: $\delta = 196.83$, 196.35 (C15,17), 187.17 (C16), 168.76 (C3), 158.63 (C1), 157.80 (C8), 154.84 (C9), 153.17 (C13), 140.08 (C11), 134.40 (C5), 128.74 (C7), 127.66 (C12), 127.35 (C10), 119.61 (C6), 117.92 (C2), 116.60 (C4), 15.63 (C14) ppm. IR: $\tilde{\nu} = 3448$ [vs, br. $\nu(\text{OH})$], 2036 (m), 1925 (s), 1901 [s $\nu(\text{CO}_{\text{fac}})$], 1626 (m), 1600 (sh.), 1566 (w), 1458 [w $\nu(\text{C}=\text{N}) + \nu(\text{C}=\text{C})$], 1270–1038 [w $\delta(\text{C}-\text{H})$] cm^{-1} . MS: m/z (%) = 588.96 (1.26) $[\text{M}]^+$, 510.05 (1.63) $[\text{M} - \text{Br}]^+$. $\text{C}_{17}\text{H}_{13}\text{BrN}_3\text{O}_4\text{Re}$ (589.42): calcd. C 34.64, H 2.22, N 7.13; found C 35.20, H 2.03, N 6.88.

Acknowledgments

This research was supported by the European Rural Development Fund, the Directorates General for Research of the Galician Government, and the Spanish Ministry of Education and Science through projects CTQ2006-05642/BQU and PGIDIT06PXIB314373PR, and by the Portuguese Foundation for Science and Technology (POCI/QUI/55519/2004 FCT/FEDER and PDTCT/QUI/66250/2006).

- [1] R. Schibli, R. Schwarzbach, R. Alberto, K. Ortner, H. Schmalte, C. Dumas, A. Egli, P. A. Schubiger, *Bioconjugate Chem.* **2002**, *13*, 750–756.
- [2] R. Alberto, K. Ortner, N. Wheatley, R. Schibli, A. P. Schubiger, *J. Am. Chem. Soc.* **2001**, *123*, 3135–3136.
- [3] J. Wald, R. Alberto, K. Ortner, L. Candrea, *Angew. Chem. Int. Ed.* **2001**, *40*, 3062–3066.

- [4] N. Metzler-Nolte, *Angew. Chem. Int. Ed.* **2001**, *40*, 1040–1043.
- [5] R. Schibli, R. La Bella, R. Alberto, E. García-Garayoa, K. Ortner, U. Abram, P. A. Schubiger, *Bioconjugate Chem.* **2000**, *11*, 345–351.
- [6] R. Waibel, R. Alberto, J. Willuda, R. Finfern, R. Schibli, A. Stichelberger, A. Egli, U. Abram, J. Mach, A. Plückerthun, P. A. Schubiger, *Nat. Biotechnol.* **1999**, *17*, 897–901.
- [7] G. Knör, M. Leirer, A. Vogler, *J. Organomet. Chem.* **2000**, *610*, 16–19.
- [8] A. Albertino, C. Garino, S. Ghiani, R. Gobetto, C. Nervi, L. Salassa, E. Rosenberg, A. Sharmin, G. Viscardi, R. Buscaino, G. Croce, M. Milanese, *J. Organomet. Chem.* **2007**, *692*, 1377–1391.
- [9] J. V. Caspar, T. J. Meyer, *J. Phys. Chem.* **1983**, *87*, 952–957.
- [10] B. J. Coe, S. Houbrechts, I. Asselberghs, A. Persoons, *Angew. Chem. Int. Ed.* **1999**, *38*, 366–369.
- [11] R. Carballo, J. S. Casas, E. García-Martínez, G. Pereiras-Gabián, A. Sánchez, J. Sordo, E. M. Vázquez-López, *Inorg. Chem.* **2003**, *42*, 6395–6403.
- [12] R. Carballo, J. S. Casas, E. García-Martínez, G. Pereiras-Gabián, A. Sánchez, J. Sordo, E. M. Vázquez-López, J. C. García-Monteagudo, *J. Organomet. Chem.* **2002**, *656*, 1–10.
- [13] R. Carballo, J. S. Casas, E. García-Martínez, G. Pereiras-Gabián, A. Sánchez, U. Abram, E. M. Vázquez-López, *CryscEngComm* **2005**, *7*, 113–120.
- [14] P. Barbazán, R. Carballo, J. S. Casas, E. García-Martínez, G. Pereiras-Gabián, A. Sánchez, E. M. Vázquez-López, *Inorg. Chem.* **2006**, *45*, 7323–7330.
- [15] J. Grewe, A. Hagenbach, B. Stromburg, R. Alberto, E. Vázquez-López, U. Abram, *Z. Anorg. Allg. Chem.* **2003**, *629*, 303–311.
- [16] G. Pereiras-Gabián, E. M. Vázquez-López, H. Braband, U. Abram, *Inorg. Chem.* **2005**, *44*, 834–836.
- [17] M. D. Cohen, G. M. J. Schmidt, S. Flavian, *J. Chem. Soc.* **1964**, 2041–2051.
- [18] F. Chen-jie, D. Chun-ying, M. Hong, H. Cheng, M. Qing-jin, L. Yong-jiang, M. Yu-hua, W. Zhe-ming, *Organometallics* **2001**, *20*, 2525–2532.
- [19] X. Xu, X. You, Z. Sun, X. Wang, H. Liu, *Acta Crystallogr. Sect. C* **1994**, *50*, 1169–1171.
- [20] W. Wang, B. Spingler, R. Alberto, *Inorg. Chim. Acta* **2003**, *355*, 386–393.
- [21] B. R. Leeflang, J. F. G. Vliegthart, L. M. J. Kroon-Batenburg, B. P. van Eijck, J. A. Kroon, *Carbohydr. Res.* **1992/614**, *230*, 41–61.
- [22] M. C. Etter, *Acc. Chem. Res.* **1990**, *23*, 120–126.
- [23] R. Alberto, R. Schibli, R. Waibel, U. Abram, A. P. Schubiger, *Coord. Chem. Rev.* **1999**, *190–192*, 901–919.
- [24] G. Desiraju, T. Steiner in *International Union of Crystallography Monographs on Crystallography, Number 9: The Weak Hydrogen Bond In Structural Chemistry and Biology*, Oxford University Press, Oxford, **2001**, p. 480.
- [25] G. R. Desiraju, A. Gavezzoti, *J. Chem. Soc., Chem. Commun.* **1989**, 621–623.
- [26] E. Hadjoudis, I. M. Mavridis, *Chem. Soc. Rev.* **2004**, *33*, 579–588.
- [27] S. M. El-Medani, M. M. Aboaly, H. H. Abdalla, R. M. Ramadan, *Spectrosc. Lett.* **2004**, *37*, 619–632.
- [28] G. A. Jeffrey in *An Introduction to Hydrogen Bonding*, Oxford University Press, New York, **1997**, p. 303.
- [29] M. St.-Jacques, P. R. Sundararajan, K. J. Taylor, R. H. Marchessault, *J. Am. Chem. Soc.* **1976**, *98*, 4386–4391.
- [30] a) A. Vogler, H. Kunkely, *Coord. Chem. Rev.* **2000**, *200–202*, 991–1008; b) B. D. Rossenaar, D. J. Stufkens, A. Vlcek Jr, *Inorg. Chem.* **1996**, *35*, 2902–2909; c) G. J. Stor, F. Hartl, J. W. M. Van Outersterp, D. J. Stufkens, *Organometallics* **1995**, *14*, 115–1131.
- [31] S. P. Schmidt, W. C. Troglor, F. Basolo, *Inorg. Synth.* **1990**, *28*, 160.
- [32] M. F. Farona, K. F. Kraus, *Inorg. Chem.* **1970**, *9*, 1700–1704.

- [33] G. M. Sheldrick, *SADABS*, University of Göttingen, Germany, **1996**.
- [34] G. M. Sheldrick, *SHELX-97: Program for the Solution and Refinement of Crystal Structures*, version 2, University of Göttingen, Germany, **1997**.
- [35] IUCr (Ed.: A. J. C. Wilson), *International Tables for Crystallography*, Kluwer, Dordrecht, **1992**, vol. C.
- [36] A. L. Spek, *PLATON: A Multipurpose Crystallographic Tool*, version 21.08.03 for LINUX, Utrecht University, Utrecht, The Netherlands, **2006**.
- [37] I. J. Bruno, J. C. Cole, P. R. Edgington, M. K. Kessler, C. F. Macrae, P. McCabe, J. Pearson, R. Taylor, *Acta Crystallogr., Sect. B* **2002**, *58*, 389–397.
- [38] U. Sandbhor, S. Padhye, D. Billington, D. Rathbone, S. Franzblau, C. E. Anson, A. K. Powell, *J. Inorg. Biochem.* **2002**, *90*, 127–136.

Received: November 7, 2007
Published Online: April 30, 2008